Energy & Environmental Science

COMMUNICATION

View Article Online
View Journal | View Issue



CrossMark click for updates

Cite this: *Energy Environ. Sci.*, 2015, **8**, 540

Received 10th October 2014
Accepted 2nd December 2014

DOI: 10.1039/c4ee03215b

www.rsc.org/ees

# Unexpected discovery of low-cost maricite $NaFePO_4$ as a high-performance electrode for Na-ion batteries†

Jongsoon Kim,‡[a] Dong-Hwa Seo,‡[b] Hyungsub Kim,[b] Inchul Park,[bc] Jung-Keun Yoo,[d] Sung-Kyun Jung,[b] Young-Uk Park,[bc] William A. Goddard III[e] and Kisuk Kang*[bc]

Battery chemistry based on earth-abundant elements has great potential for the development of cost-effective, large-scale energy storage systems. Herein, we report, for the first time, that maricite $NaFePO_4$ can function as an excellent cathode material for Na ion batteries, an unexpected result since it has been regarded as an electrochemically inactive electrode for rechargeable batteries. Our investigation of the Na re-(de)intercalation mechanism reveals that all Na ions can be deintercalated from the nano-sized maricite $NaFePO_4$ with simultaneous transformation into amorphous $FePO_4$. Our quantum mechanics calculations show that the underlying reason for the remarkable electrochemical activity of $NaFePO_4$ is the significantly enhanced Na mobility in the transformed phase, which is ~one fourth of the hopping activation barrier. Maricite $NaFePO_4$, fully sodiated amorphous $FePO_4$, delivered a capacity of 142 mA h $g^{-1}$ (92% of the theoretical value) at the first cycle, and showed outstanding cyclability with a negligible capacity fade after 200 cycles (95% retention of the initial cycle).

**Broader context**

We report, for the first time, that maricite $NaFePO_4$ can function as an excellent cathode material for Na ion batteries, an unexpected result since it has been regarded as an electrochemically inactive electrode for rechargeable batteries. Our investigation of the Na re-(de)intercalation mechanism reveals that all Na ions can be deintercalated from the nano-sized maricite $NaFePO_4$ with simultaneous transformation into amorphous $FePO_4$. Our quantum mechanics calculations show that the underlying reason for the remarkable electrochemical activity of $NaFePO_4$ is the significantly enhanced Na mobility in the transformed phase, which is ~one fourth of the hopping activation barrier. Maricite $NaFePO_4$, fully sodiated amorphous $FePO_4$, delivered a capacity of 142 mA h $g^{-1}$ (92% of the theoretical value) at the first cycle, and showed outstanding cyclability with a negligible capacity fade after 200 cycles (95% retention of the initial cycle).

The demand for large-scale energy storage systems (EESs) has prompted considerable effort in the development of new types of batteries with cost-effective and sustainable properties. While the high cost of current Li ion batteries (LIBs) remains one of the major hurdles towards large-scale energy storage applications,[1–12] battery chemistry based on earth-abundant elements offers a feasible solution. Recently, Na ion batteries (NIBs) have been considered as a promising alternative to LIBs since the underlying electrochemical reaction is similar to that of LIBs, but is based on the unlimited resources of Na from seawater.[13–20] The use of redox chemistry using earth abundant transition metals would provide the optimal combination with Na electrochemistry further highlighting the advantage of NIBs.

In recent years, considerable research has been carried out on Fe-based electrode materials for use in NIBs.[16,19,21–24] Komaba *et al.* reported a series of layered $Na(Fe,Mn)O_2$ cathodes exhibiting promising electrochemical properties.[16] Nazar *et al.*, Yamada *et al.*, and Choi *et al.* showed that the reversible intercalation of Na ions with the $Fe^{2+}/Fe^{3+}$ redox reactions is possible in polyanionic compounds, such as $Na_2FePO_4F$ and $Na_2FeP_2O_7$.[20,22,23,25] More recently, our group reported $Na_4Fe_3(PO_4)_2(P_2O_7)$, a mixed-polyanionic compound as a new cathode for NIBs. In particular, such polyanionic compounds are capable of accommodating large Na ions in the crystal with only slight volumetric changes, thus behaving as stable reversible hosts for Na ions. Furthermore, the stable P–O covalent bond offers chemical and structural stability, even though the heavy framework generally reduces the theoretical capacity. Herein,

[a]*Korea Atomic Energy Research Institute (KAERI), P. O. Box 105, Yuseong-gu, Daejeon 305-600, Korea*

[b]*Department of Materials Science and Engineering, Research Institute of Advanced Materials, Seoul National University, 599 Gwanak-ro, Gwanak-gu, Seoul 151-742, Korea. E-mail: matlgen1@snu.ac.kr*

[c]*Center for Nanoparticle Research, Institute for Basic Science, Seoul National University, Seoul 151-742, Korea*

[d]*Department of Materials Science and Engineering, Korea Advanced Institute of Science and Technology (KAIST), 291 Daehak-ro, Yuseong-gu, Daejeon 305-701, Korea*

[e]*Materials and Process Simulation Center (MC 139-74), California Institute of Technology, 1200 East California Boulevard, Pasadena, CA, 91125, USA*

† Electronic supplementary information (ESI) available. See DOI: 10.1039/c4ee03215b

‡ Jongsoon Kim and Dong-Hwa Seo equally contributed to this manuscript.

we introduce $NaFePO_4$ as a promising cathode material for NIBs. Although its theoretical capacity (*ca.* 155 mA h $g^{-1}$) can far exceed other reported Fe-based polyanion cathode materials, such as $Na_2FePO_4F$ (*ca.* 120 mA h $g^{-1}$), $Na_2FeP_2O_7$ (*ca.* 90 mA h $g^{-1}$) and $Na_4Fe(PO_4)_2(P_2O_7)$ (*ca.* 130 mA h $g^{-1}$),[17–22,26] maricite, the thermodynamically stable phase of $NaFePO_4$, has been regarded as electrochemically inactive in rechargeable batteries.[20] The $NaFePO_4$ composition also exhibits an olivine structure; however, the olivine structure is not stable and cannot be synthesized by conventional synthetic routes.[17–19] In this work, we show, for the first time, that maricite $NaFePO_4$ can function as an excellent cathode material for rechargeable Na batteries.

We synthesized maricite $NaFePO_4$ powder through a simple solid-state method followed by ball-milling with conductive carbon. X-ray diffraction (XRD) and transmission electron microscopy (TEM) analyses (ESI Fig. S1†) show that maricite $NaFePO_4$ (particle size: *ca.* 50 nm) is phase-pure, *i.e.*, without any impurities or second phases. It is identified that the amount of carbon in the carbon-mixed $NaFePO_4$ is approximately 20%, using thermo-gravimetric analysis (TGA) and carbon analysis (ESI Fig. S2 and ESI Table 1†). Details regarding the experimental conditions are provided in the ESI.† We first investigated the electrochemical activity of maricite $NaFePO_4$ in Na cells using a Na metal anode with a 1 M $NaPF_6$ (1 : 1 EC/PC) electrolyte. To our surprise, a maricite $NaFePO_4$ electrode could be charged and discharged with almost all Na ions participating in the electrochemical reaction (Fig. 1(a)). At a C/20 rate, we observed a capacity of *ca.* 142 mA h $g^{-1}$, which corresponds to 92% of its theoretical capacity. In our comparative study with lithium cells, we also found that a similar mechanism works for the maricite electrode with lithium (ESI Fig. S3†). During the first charge, Na is extracted from the maricite showing a slightly high charging voltage, followed by amorphization. After the transition, the electrochemical profile becomes similar to the well-known behavior of the amorphous $FePO_4$ in the lithium cells.[27,28] Moreover, this capacity was retained over more than 200 cycles (Fig. 1(b)) without a notable change in the electrochemical profile with the exception of the first charge curve. The inset of Fig. 1(a) shows the discharge profiles of the maricite $NaFePO_4$ electrode measured at various current rates (2 C, 1 C, C/2, C/5, C/10, and C/20 from 1.5 to 4.5 V), which indicates that *ca.* 70% of the initial capacity can be delivered in 1.288 hour (C/2 rate) and that *ca.* 60% of the initial capacity can be delivered even in 0.552 hour (1 C rate), indicating that this electrode can sustain respectable rate capabilities. Our experimental data show that Na extraction/insertion can be reversible in the maricite $NaFePO_4$ electrode, which is contrary to the conventional belief that the lack of feasible diffusion pathways of Na ions in maricite $NaFePO_4$ should make it electrochemically inactive.

The maricite crystal structure has the same anionic framework as olivine; however, the M1 and M2 cation site occupations are completely reversed. For example, in olivine $LiFePO_4$, the M1 sites are fully occupied by $Li^+$, while $Fe^{2+}$ occupies the M2 sites. In contrast for maricite, $Fe^{2+}$ atoms are in M1 sites, while $Na^+$ occupies all the M2 sites. Due to the long distance between M2 sites in maricite, it has been assumed that Na hopping between sites is not plausible.[29] Indeed we carried out our Quantum Mechanics (QM) calculations (the PBE flavour of Density Functional Theory, DFT) confirming that extracting Na ions from the maricite $NaFePO_4$ structure would be almost impossible under typical battery operating conditions (Fig. 2). Thus using the nudged elastic band (NEB) method in QM calculations, we find that diffusion of Na ions in maricite $Na_{1-x}FePO_4$ ($x \approx 0$) can proceed *via* two most plausible paths: path 1 in the *bc* plane and path 2 along the *b* direction as shown in Fig. 2(a). However, we calculate an activation barrier for Na hopping along path 1 to be ~1.46 eV and that along path 2 is ~1.79 for Li or Na hopping in conventional battery materials ranging between 0.2 and 0.6 eV;[30–32] the diffusivity of Na in maricite would likely be several orders of magnitude lower, making Na diffusion quite unlikely at room temperature.[33] Without the creation of a new path having far lower activation barriers for Na diffusion, Na ions could not be extracted from the electrode materials.

This expectation from the QM is directly contradicted by our experiments. While carrying out experimental studies to explain

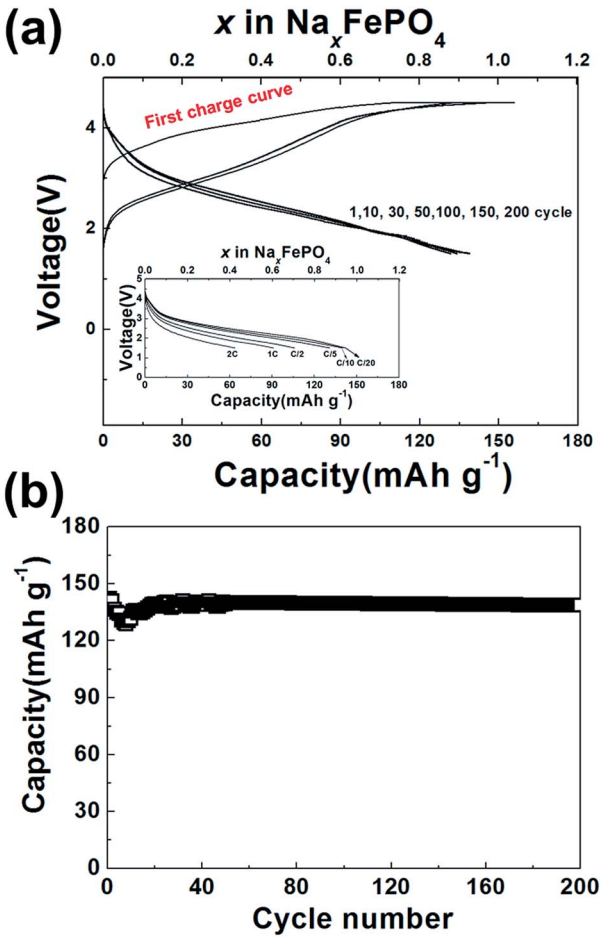


Fig. 1 (a) Galvanostatic curves of maricite $NaFePO_4$ over 200 cycles at C/20 in a Na cell [inset: discharge curves of maricite $NaFePO_4$ as a function of the C rate from C/20 to 3 C (charging under CCCV mode (C/20 rate and 5 hour holding at 4.5 V)), during the first charge of CV, 20 mA h $g^{-1}$ of capacity was recovered and (b) cyclability of maricite $NaFePO_4$ over 200 cycles at C/20 in a Na cell.

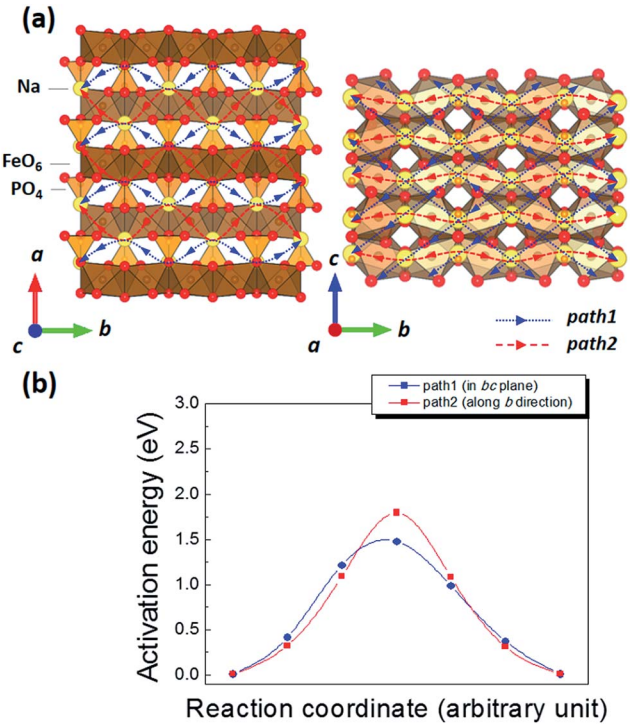


Fig. 2 (a) Na diffusion pathways in maricite $NaFePO_4$ and (b) activation barriers for Na hopping along two diffusion pathways of maricite $NaFePO_4$.

this discrepancy, we observed that the shape and voltage of the first charge curve are always clearly different from the subsequent charge–discharge profiles in Fig. 1(a). This indicates that the desodiation of maricite may have induced a transformation into a different desodiated phase.[34–36] To probe possible phase transformations of the maricite structure, we carried out QM calculations to compare the formation energies of various $Na_xFePO_4$ phases including olivine $NaFePO_4$, $FePO_4$, maricite $NaFePO_4$ and $FePO_4$. As shown in ESI Table S2,† we found that the olivine $FePO_4$ is more stable than maricite $FePO_4$ by 30 meV per formula unit, while $NaFePO_4$ is more stable in the maricite structure than in the olivine structure. This indicates that desodiating $Na_xFePO_4$ provides a driving force for the maricite structure to undergo a phase transformation during desodiation. To confirm the phase transformation of the desodiated phase, we prepared fully desodiated maricite $FePO_4$ (detailed conditions of desodiation and the analysis are in the ESI and ESI Table S3†). However, XRD measurements showed no peaks after desodiation, Fig. 3(a), indicating the formation of an amorphous structure.

Furthermore, the *ex situ* electrochemical desodiation in Fig. 3(b) shows that the intensity of the XRD peaks of maricite $NaFePO_4$ gradually decreases with charging, suggesting the loss of long-range order and the amorphization of the maricite crystal. Any growth or change of peaks was not observed in the XRD pattern when Na ions are fully re-inserted into the structure (discharging at 1.5 V). Moreover, the extended X-ray absorption fine structure (EXAFS) measurements, Fig. 3(c), reveal a pattern similar to that of amorphous $FePO_4$ (denoted as

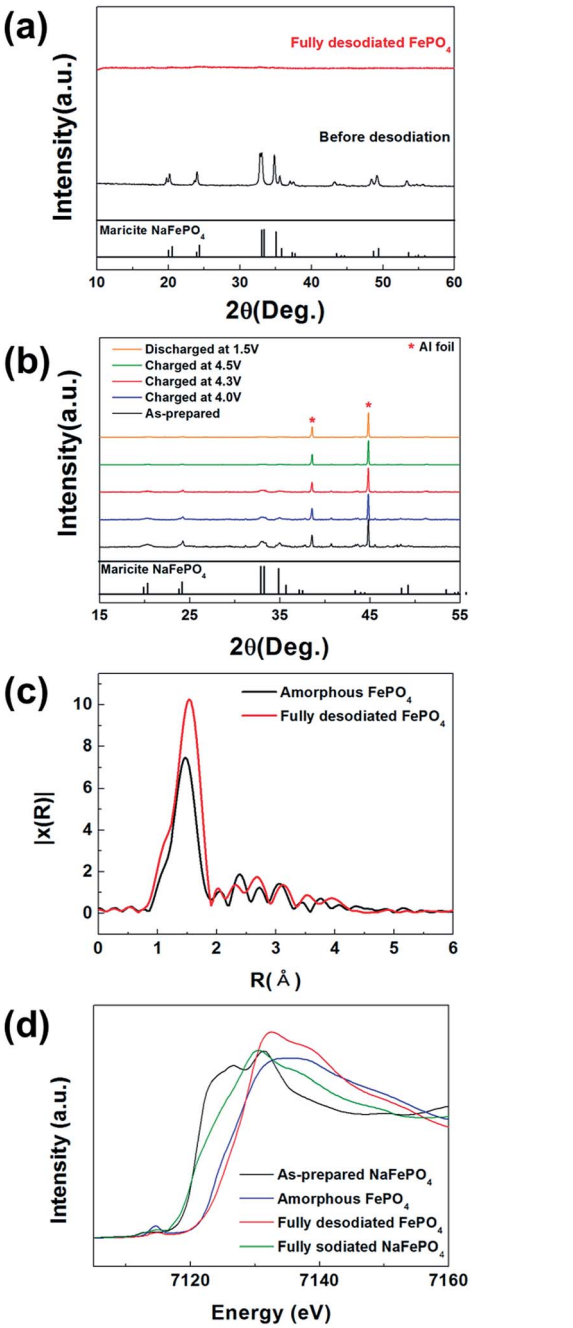


Fig. 3 (a) XRD pattern of fully desodiated maricite $FePO_4$, (b) *ex situ* XRD patterns of maricite $Na_xFePO_4$ during the first charge (*: Al Foil), (c) normalized Fe EXAFS spectra of fully desodiated maricite $NaFePO_4$ and a-$FePO_4$, and (d) normalized Fe XANES spectra of as-prepared $NaFePO_4$, fully desodiated maricite $FePO_4$, re-sodiated maricite $NaFePO_4$, and a-$FePO_4$.

a-$FePO_4$), indicating that the long-range order is lost. We conclude that the first desodiation transforms maricite into the amorphous phase rather than into an energetically more favourable olivine structure, probably due to kinetic limitations of Fe atoms to migrate at room temperature. We expect that this incomplete motion of Fe atoms to form olivine may have caused significant disordering of the crystal resulting in the formation of the amorphous phase. Even so, the X-ray absorption near

 

edge structure (XANES) analysis indicates that reversible $Fe^{2+}/Fe^{3+}$ redox reactions still occur in the electrode during charge/discharge cycling (Fig. 3(d)).

We used QM to investigate how Na ions can be reversibly deintercalated (intercalated) from (into) the $Na_xFePO_4$ structure after amorphization of the crystal structure. Ion diffusion in amorphous structures is generally tricky to grasp with QM calculations due to the lack of long-range order. The absence of atomic order in the amorphous material complicates the identification of representative diffusion pathways. Consequently, we adopted a new multi-scale computational method to evaluate Na diffusion in the amorphous $FePO_4$. We, first, constructed an amorphous structure of $FePO_4$ by melting and then quenching rapidly using QM molecular dynamics (MD) simulations (that is MD using QM to calculate the forces) (ESI Fig. S4 and S5†).[37,38] Here we used grand canonical Monte Carlo (GCMC) simulations to identify, stable Na sites in a-$FePO_4$.[39] We then examined diffusion pathways between these stable Na sites in a-$FePO_4$ using the bond valence summation (BVS) method.[40,41] The activation energies for Na hopping through these diffusion pathways were then obtained from QM based NEB calculations.[42] Fig. 4(a) illustrates the plausible Na sites and diffusion paths in a-$FePO_4$. The coordination numbers of Na ions vary from 4 to 7 in a-$FePO_4$, whereas the coordination number is 6 in olivine $FePO_4$ or maricite $FePO_4$. We found that the diffusion pathways of a-$FePO_4$ are random and disordered, compared with olivine $FePO_4$, which has a one-dimensional diffusion tunnel along the *b* direction (ESI Fig. S6†). Because there are no representative diffusion pathways, we statistically evaluated the activation energies of Na hopping between neighbouring Na sites in three a-$FePO_4$ structures constructed independently by the melt-and-quenching process. The activation energies for Na hopping in a-$FePO_4$ ranged from 0.16 to 1.06 eV, as shown in Fig. 4(b). Indeed these values are much lower than that in maricite $Na_{1-x}FePO_4$ (*ca.* 2.68 eV for $x \approx 1$) (ESI Fig. S7†), although some are higher than that in olivine $FePO_4$ (*ca.* 0.28 eV).[43] We also evaluated the activation energies for Na diffusion along long pathways (>1 nm) to capture a realistic picture of Na motion in the disordered structure of a-$FePO_4$. The overall activation energy along Na1–Na2–Na3–Na4/Na5 (~1 nm) was ~0.73 eV. This value is still much lower than that in maricite $Na_{1-x}FePO_4$ ($x \approx 1$, *ca.* 2.68 eV). For comparison, we estimated the activation energy for Li hopping in a-$FePO_4$ using the same computational scheme. This resulted in an activation energy of ~0.45 eV, which is comparable to that of other crystalline Li cathode materials (0.25–0.5 eV). These results indicate that a-$FePO_4$ could be a suitable electrode for LIBs (ESI Fig. S8†).[27,28] We expect that the slightly higher activation energy for Na hopping compared to Li in a-$FePO_4$ is due to the larger ionic size of the Na ion. This difference is in line with that of the activation energies for Na and Li ions in olivine $FePO_4$ (0.280 *vs.* 0.165 eV).[43] Nevertheless, we expect that the reduction of the activation barrier for Na hopping by ~75% (from *ca.* 2.68 to *ca.* 0.73 eV) through amorphization of the maricite will increase Na diffusion by tens of orders of magnitudes, allowing Na diffusion under normal battery operating conditions. T. Shiratsuchi *et al.* demonstrated that the amorphous $FePO_4$ can show better electrochemical behavior than those of the trigonal crystalline $FePO_4$ structure by comparing the electrochemical performance between amorphous $FePO_4$ and trigonal $FePO_4$. This report is in excellent agreement with our observation that the electrochemical properties of the maricite $NaFePO_4$ have been remarkably enhanced by the simultaneous phase transition to the amorphous phase.

In Fig. 4(d), we propose the electrochemical mechanism of maricite $NaFePO_4$. When Na ions at the surface are extracted from the structure, maricite $FePO_4$ simultaneously transforms into a-$FePO_4$ (two-phase reaction, it was clearly confirmed by TEM analyses as shown in Fig. 5). Through new fast diffusion pathways in a-$FePO_4$, the Na ions in the inner portion of maricite $FePO_4$ are further deintercalated, transforming into a-$FePO_4$. After all Na ions are extracted and maricite $FePO_4$ has turned fully into a-$FePO_4$, subsequent electrochemical cycles proceed by reversible insertion/extraction of Na ions through a-$FePO_4$ (solid-solution reaction). We have performed the galvanostatic intermittent titration technique (GITT) measurement in particular during the first charge process, where the conversion from the maricite to the amorphous phase is expected to occur (ESI Fig. S9†). In this measurement we slowly charged the sample with a current density of 7.75 mA $g^{-1}$ and relaxed until the voltage converges within $dV/dt \sim 10^{-6}$ V $s^{-1}$. From the GITT measurement below, it is shown that the relaxed voltage follows the constant value with respect to the state of the charge indicating that the transformation from maricite $NaFePO_4$ to amorphous $FePO_4$ is based on a two-phase reaction

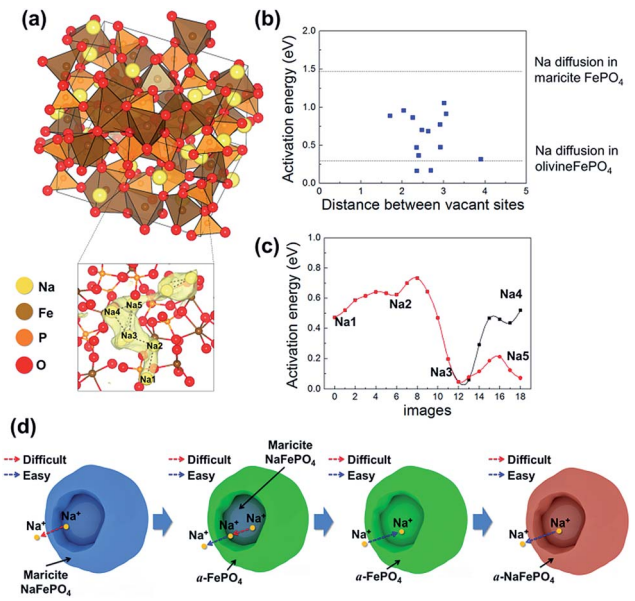


Fig. 4 Na diffusion in a-$FePO_4$. (a) Plausible Na sites and diffusion pathways of a-$FePO_4$, (b) activation energies of Na hopping between Na sites as a function of distance between Na sites, and (c) the activation energies for Na diffusion along Na1–Na2–Na3–Na4/Na5 diffusion pathways (over 10 Å) in a-$FePO_4$. The dashed lines indicate the activation energies of Na diffusion in olivine $FePO_4$ and maricite $FePO_4$. (d) Schematic representation of the electrochemical mechanism during charge/discharge cycling in maricite $NaFePO_4$.

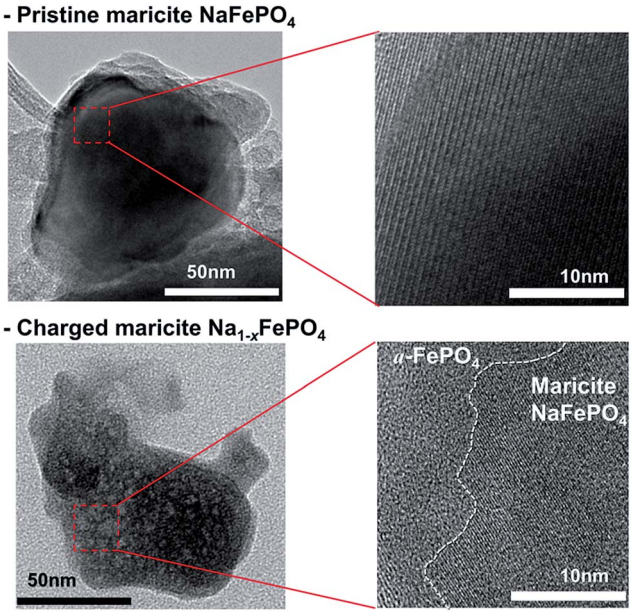


Fig. 5 Comparison of TEM images between pristine maricite $NaFePO_4$ and partially charged maricite $Na_{1-x}FePO_4$. It confirmed the two-phase reaction at transformation from maricite $NaFePO_4$ to a-$FePO_4$ during the first charge.

despite the seemingly sloppy profile during the first charge process.

It clearly suggests that the first desodiation from the maricite $NaFePO_4$ leads to the nucleation and growth of the amorphous $FePO_4$. It also indicates that the subsequent discharge and charge is purely based on the electrochemical properties of the amorphous $FePO_4$. Previous reports on the amorphous $FePO_4$ electrode have demonstrated that a solid-solution behavior is observed in the charge/discharge of the $FePO_4$.[27,28,44] Thus after the maricite $NaFePO_4$ transforms into a-$FePO_4$, it can remain in the sodiated a-$FePO_4$ structure. We note that the initial containment of Na in the maricite $NaFePO_4$ can be a great advantage in the utilization of NIBs, since it is very stable until after the first cycle. This way we can avoid starting with the metallic Na anode, which poses a potential safety risk. Furthermore, recently discovered high performance anode materials such as P, Sn, and Sb would require Na containing cathode materials.[45–48] In this respect, a-$FePO_4$ is not suitable in spite of its promising electrochemical activity with Na and necessitates a pre-sodiation step either by chemical or electrochemical ways.

## Conclusions

In summary, we combined QM calculations and experiments to identify the electrochemical mechanism responsible for the electrochemical activity of maricite $NaFePO_4$. Despite the general perception that maricite $NaFePO_4$ is electrochemically inactive, remarkable battery performance of the maricite $NaFePO_4$ electrode in NIBs was demonstrated. We find that the first deintercalation of Na ions transforms maricite $FePO_4$ into a-$FePO_4$ as shown by XRD and EXAFS analyses. Our QM calculations show that the transformation into a-$FePO_4$ is the key step for reversible Na de/intercalation in the electrode. This is because a-$FePO_4$ allows substantially smaller barriers than maricite $NaFePO_4$ for Na to hop from site to site. We predict that fully desodiated maricite $NaFePO_4$ forms amorphous $FePO_4$, providing a potential candidate for low-cost Na ion battery cathodes.

## Acknowledgements

This work was supported by the World Premier Materials grant funded by the Korea government Ministry of Trade, Industry and Energy and the Human Resources Development program (20124010203320) of the Korea Institute of Energy Technology Evaluation and Planning (KETEP) grant funded by the Korea government Ministry of Trade, Industry and Energy.

## Notes and references

1 J. Wang, N. Yang, H. Tang, Z. Dong, Q. Jin, M. Yang, D. Kisailus, H. Zhao, Z. Tang and D. Wang, *Angew. Chem.*, 2013, **52**, 6417–6420.
2 K. Kang, Y. S. Meng, J. Breger, C. P. Grey and G. Ceder, *Science*, 2006, **311**, 977–980.
3 M. Armand and J. M. Tarascon, *Nature*, 2008, **451**, 652–657.
4 J. M. Tarascon and M. Armand, *Nature*, 2001, **414**, 359–367.
5 M. R. Palacin, *Chem. Soc. Rev.*, 2009, **38**, 2565–2575.
6 C. Delacourt, P. Poizot, J.-M. Tarascon and C. Masquelier, *Nat. Mater.*, 2005, **4**, 254–260.
7 P. S. Herle, B. Ellis, N. Coombs and L. F. Nazar, *Nat. Mater.*, 2004, **3**, 147–152.
8 J. Kim, D. H. Seo, S. W. Kim, Y. U. Park and K. Kang, *Chem. Commun.*, 2010, **46**, 1305–1307.
9 S. Y. Chung, J. T. Bloking and Y. M. Chiang, *Nat. Mater.*, 2002, **1**, 123–128.
10 J. Kim, H. Kim, I. Park, Y. U. Park, J. K. Yoo, K. Y. Park, S. Lee and K. Kang, *Energy Environ. Sci.*, 2013, **6**, 830–834.
11 S. Xu, C. M. Hessel, H. Ren, R. Yu, Q. Jin, M. Yang, H. Zhao and D. Wang, *Energy Environ. Sci.*, 2014, **7**, 632–637.
12 X. Lai, J. E. Halpert and D. Wang, *Energy Environ. Sci.*, 2012, **5**, 5604–5618.
13 R. A. Shakoor, D. H. Seo, H. Kim, Y. U. Park, J. Kim, S. W. Kim, H. Gwon, S. Lee and K. Kang, *J. Mater. Chem.*, 2012, **22**, 20535–20541.
14 S. W. Kim, D. H. Seo, X. H. Ma, G. Ceder and K. Kang, *Adv. Energy Mater.*, 2012, **2**, 710–721.
15 Z. L. Jian, W. Z. Han, X. Lu, H. X. Yang, Y. S. Hu, J. Zhou, Z. B. Zhou, J. Q. Li, W. Chen, D. F. Chen and L. Q. Chen, *Adv. Energy Mater.*, 2013, **3**, 156–160.
16 N. Yabuuchi, M. Kajiyama, J. Iwatate, H. Nishikawa, S. Hitomi, R. Okuyama, R. Usui, Y. Yamada and S. Komaba, *Nat. Mater.*, 2012, **11**, 512–517.
17 M. Casas-Cabanas, V. V. Roddatis, D. Saurel, P. Kubiak, J. Carretero-Gonzalez, V. Palomares, P. Serras and T. Rojo, *J. Mater. Chem.*, 2012, **22**, 17421–17423.

18 S. M. Oh, S. T. Myung, J. Hassoun, B. Scrosati and Y. K. Sun, *Electrochem. Commun.*, 2012, **22**, 149–152.
19 K. T. Lee, T. N. Ramesh, F. Nan, G. Botton and L. F. Nazar, *Chem. Mater.*, 2011, **23**, 3593–3600.
20 B. L. Ellis, W. R. M. Makahnouk, Y. Makimura, K. Toghill and L. F. Nazar, *Nat. Mater.*, 2007, **6**, 749–753.
21 Y. Kawabe, N. Yabuuchi, M. Kajiyama, N. Fukuhara, T. Inamasu, R. Okuyama, I. Nakai and S. Komaba, *Electrochem. Commun.*, 2011, **13**, 1225–1228.
22 P. Barpanda, T. Ye, S. Nishimura, S. C. Chung, Y. Yamada, M. Okubo, H. S. Zhou and A. Yamada, *Electrochem. Commun.*, 2012, **24**, 116–119.
23 H. Kim, R. A. Shakoor, C. Park, S. Y. Lim, J. S. Kim, Y. N. Jo, W. Cho, K. Miyasaka, R. Kahraman, Y. Jung and J. W. Choi, *Adv. Funct. Mater.*, 2013, **23**, 1147–1155.
24 T. Shiratsuchi, S. Okada, J. Yamaki and T. Nishida, *J. Power Sources*, 2006, **159**, 268–271.
25 B. L. Ellis, W. R. M. Makahnouk, W. N. Rowan-Weetaluktuk, D. H. Ryan and L. F. Nazar, *Chem. Mater.*, 2010, **22**, 1059–1070.
26 H. Kim, I. Park, S. Lee, H. Kim, K.-Y. Park, Y.-U. Park, H. Kim, J. Kim, H.-D. Lim, W.-S. Yoon and K. Kang, *Chem. Mater.*, 2013, **25**, 3614–3622.
27 Y. J. Lee, H. Yi, W. J. Kim, K. Kang, D. S. Yun, M. S. Strano, G. Ceder and A. M. Belcher, *Science*, 2009, **324**, 1051–1055.
28 S.-W. Kim, J. Ryu, C. B. Park and K. Kang, *Chem. Commun.*, 2010, **46**, 7409–7411.
29 R. Shakoor, Y.-U. K. Park, J. Kim, S.-W. Kim, D.-H. Seo, H. Gwon and K. Kang, *J. Korean Battery Soc.*, 2010, **3**, 00–00.
30 A. Van der Ven, G. Ceder, M. Asta and P. D. Tepesch, *Phys. Rev. B: Condens. Matter Mater. Phys.*, 2001, **64**, 184307.
31 D. Morgan, A. Van der Ven and G. Ceder, *Electrochem. Solid-State Lett.*, 2004, **7**, A30–A32.
32 S. P. Ong, V. L. Chevrier, G. Hautier, A. Jain, C. Moore, S. Kim, X. Ma and G. Ceder, *Energy Environm. Sci.*, 2011, **4**, 3680–3688.
33 D.-H. Seo, Y.-U. Park, S.-W. Kim, I. Park, R. A. Shakoor and K. Kang, *Phy. Rev. B*, 2011, **83**, 205127.
34 D. H. Seo, H. Kim, I. Park, J. Hong and K. Kang, *Phy. Rev. B*, 2011, **84**, 220106.
35 D. P. Lv, J. Y. Bai, P. Zhang, S. Q. Wu, Y. X. Li, W. Wen, Z. Jiang, J. X. Mi, Z. Z. Zhu and Y. Yang, *Chem. Mater.*, 2013, **25**, 2014–2020.
36 C. Eames, A. R. Armstrong, P. G. Bruce and M. S. Islam, *Chem. Mater.*, 2012, **24**, 2155–2161.
37 P. Ballone, W. Andreoni, R. Car and M. Parrinello, *Phys. Rev. Lett.*, 1988, **60**, 271–274.
38 K. Jarolimek, R. A. de Groot, G. A. de Wijs and M. Zeman, *Phys. Rev. B: Condens. Matter Mater. Phys.*, 2009, **79**, 155206.
39 D.-H. Seo, H. Kim, H. Kim, W. A. Goddard, III and K. Kang, *Energy Environ. Sci.*, 2011, **4**, 4938–4941.
40 I. D. Brown, in *Structure and Bonding in Crystals 2*, 1981, pp. 1–30.
41 M. Sale and M. Avdeev, *J. Appl. Crystallogr.*, 2012, **45**, 1054–1056.
42 G. M. H. Jonsson, K. W. Jacobsen and B. J. Berne, in *Classical and Quantum Dynamics in Condensed Phase Simulations*, World Scientific, 1998.
43 S. P. Ong, V. L. Chevrier, G. Hautier, A. Jain, C. Moore, S. Kim, X. H. Ma and G. Ceder, *Energy Environ. Sci.*, 2011, **4**, 3680–3688.
44 Y. S. Hong, K. S. Ryu, Y. J. Park, M. G. Kim, J. M. Lee and S. H. Chang, *J. Mater. Chem.*, 2002, **12**, 1870–1874.
45 Y. Kim, Y. Park, A. Choi, N.-S. Choi, J. Kim, J. Lee, J. H. Ryu, S. M. Oh and K. T. Lee, *Adv. Mater.*, 2013, **25**, 3045–3049.
46 W.-J. Li, S.-L. Chou, J.-Z. Wang, H.-K. Liu and S.-X. Dou, *Nano Lett.*, 2013, **13**, 5480–5484.
47 I. Meschini, F. Nobili, M. Mancini, R. Marassi, R. Tossici, A. Savoini, M. L. Focarete and F. Croce, *J. Power Sources*, 2013, **226**, 241–248.
48 L. Wu, X. Hu, J. Qian, F. Pei, F. Wu, R. Mao, X. Ai, H. Yang and Y. Cao, *Energy Environ. Sci.*, 2014, **7**, 323–328.